

Article

Development of a Natural Matrix Hybrid Hydrogel Patch and Evaluation of Its Efficacy against Atopic Dermatitis

Gyeong Sik Hong ^{1,†}, Jeong Yeon Choi ^{2,†}, Jang Soo Suh ³, Jeong Ok Lim ⁴ and Jin Hyun Choi ^{1,*} 

¹ Department of Biofibers and Biomaterials Science, Kyungpook National University, Daegu 41566, Korea; gshong0625@naver.com

² Safety System R&D Group, Korea Institute of Industrial Technology (KITECH), Daegu 42994, Korea; jychoi77@kitech.re.kr

³ Department of Laboratory Medicine, Kyungpook National University School of Medicine, Kyungpook National University Hospital, Daegu 41944, Korea; suhjs@knu.ac.kr

⁴ Biomedical Research Institute, Joint Institute for Regenerative Medicine, Kyungpook National University School of Medicine, Kyungpook National University Hospital, Daegu 41944, Korea; jolim@knu.ac.kr

* Correspondence: jinhchoi@knu.ac.kr; Tel.: +82-53-950-5740

† These authors are contributed equally to the work as first authors.

Received: 27 October 2020; Accepted: 2 December 2020; Published: 7 December 2020



Abstract: Although there is no cure for atopic dermatitis (AD), treatments to relieve AD symptoms are available. A previously developed topical patch for AD treatment minimizes skin irritation but does not sufficiently adhere and absorb to specific areas. *Centella asiatica* extract (CAE) is a natural polymer for atopic treatment. This study fabricated a CAE-loaded hyaluronic acid-dextran (HA-Dex) hybrid hydrogel patch for use as an AD treatment and evaluated the effect of varying CAE concentrations in the patch. The CAE-loaded HA-Dex hybrid hydrogel patch was fabricated into a sheet-type scaffold using a freeze-drying process and 1,4-butanediol diglycidyl ether (BDDE). Fibroblasts (L929 cells) were used to evaluate cell survival, and physical properties were evaluated using Fourier transform infrared spectroscopy, field emission scanning electron microscopy, a universal testing machine, and high-performance liquid chromatography. A 0.4 wt% CAE-loaded HA-Dex hybrid hydrogel patch produced the most stable release profile and the highest level of cellular activity. These hydrogel patches provided moisture and released CAE over an extended period of time, making them ideal for relieving atopic itching. This delivery system enables the extended release of CAE to localized areas and could potentially be used to apply a variety of products to treat AD.

Keywords: atopic dermatitis treatment; hydrogel patch; hyaluronic acid; dextran; *Centella asiatica* extract

1. Introduction

In cases of atopic dermatitis (AD), genetic and acquired factors damage the skin barrier but the cause of AD is unknown [1]. AD is classified into infant, pediatric, and adult types according to onset age. Furthermore, acute, subacute, and chronic AD exhibit different symptoms as well as varying lesion types and distribution. AD is a representative disease of childhood and adolescence that is most often observed in infants and children and can develop into a chronic, recurrent, inflammatory skin disease. Symptoms begin around 100 days after birth in infants. Dry skin, erythema (skin redness), and scales (white debris) improve and worsen in a cycle that results in a malfunction of the barrier formed by the skin. This allows harmful external substances to easily penetrate the skin; these allergic irritants that invade the skin cause AD [2,3].

Currently, there is no cure for AD. However, several researchers have suggested basic methods to protect the skin and identify and remove inducers of AD, as well as treatments to supply moisture to the skin and reduce itchiness. Topical steroids and local calcineurin inhibitors are the most commonly used drug treatments. Although topical steroids have a strong effect, the use of steroid ointments and creams leads to excessive immune response suppression that can result in pathogen propagation that may exacerbate skin infections [4]. Furthermore, steroid ointments inhibit collagen synthesis; overuse may decrease the collagen layer of the skin and result in atrophy and thinner skin [5]. Continued skin blood vessel dilation (in which the skin turns red and blood vessels are visible to the naked eye) may lead to side effects such as vasodilation, skin irritation, rashes, and swelling [6].

The lack of therapeutic drug treatments for AD has resulted in the exploration of natural resources to alleviate AD symptoms and minimize side effects, even when used for extended periods. Several studies have reported that AD symptoms improve after using various medicinal materials including herbal, headworm, and *Opuntia humifusa* extracts [7,8]. *Centella asiatica* extract (CAE) effectively promotes wound regeneration and eliminates the appearance of acne scars by reducing pigmentation. Moreover, it promotes cell proliferation, collagen synthesis, and fibronectin production, which helps to increase pore elasticity and shrink pores [9]. Other studies have shown that it is effective in preventing fine wrinkles and treating eczema, as well as relieving the itching and repairing the damaged skin associated with AD [10,11]. However, an appropriate concentration of CAE must be used as excessive CAE may lead to hypertrophic scarring that remains when recovering from keloid inflammation.

Despite this, innovative treatments for AD are still lacking. Since AD is sensitive to skin irritation, the development of patches that can effectively adhere to and be absorbed in a localized area to release therapeutic treatments with minimal skin irritation should be a priority [12,13]. The materials and manufacturing methods used to form hydrogels must be carefully chosen to meet specific criteria such as binding affinity, biomaterial toxicity, and biocompatibility. Furthermore, materials with an extracellular matrix are essential for tissue regeneration. Dextran (Dex) [14] and hyaluronic acid (HA) [15,16] are widely used as drug delivery materials. HA is generally water soluble; however, HA must be insoluble in aqueous solutions for cells to attach to it. Therefore, HA must be chemically modified to enable its use as a cell scaffold despite its excellent biocompatibility and ability to promote angiogenesis [16].

To solve these problems, this study aimed to develop a new hydrogel formulation that can effectively control the release of therapeutic agents to specific local areas with minimal skin irritation. HA and Dex were mixed with a crosslinking agent, 1,4-butanediol diglycidyl ether (BDDE), to develop HA-Dex hybrid hydrogel patches. CAE, a natural product with excellent functional and physiological activities, was embedded in the patches (Figure 1). The CAE-embedded HA-Dex hybrid hydrogel patch was fabricated into a sheet-type scaffold by using a freeze-drying process and 1,4-butanediol diglycidyl ether (BDDE). Fibroblasts (L929 cells) were used to evaluate cell survival, and Fourier transform infrared spectrometry, field emission scanning electron microscopy, mechanical testing, high-performance liquid chromatography, and porosity analysis were used to analyze physical properties.

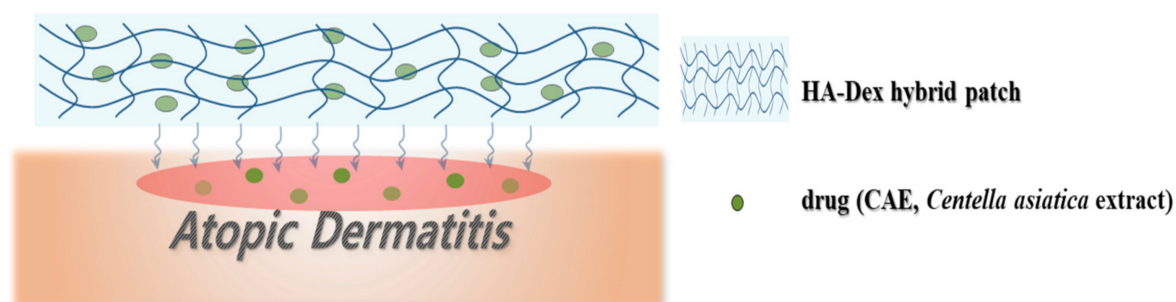


Figure 1. Concept of atopic dermatitis treatment using a *Centella asiatica* extract (CAE)-loaded hyaluronic acid (HA)-dextran (Dex) hybrid hydrogel patch.

2. Materials and Methods

2.1. Manufacturing Method

HA-Dex hybrid patches were prepared using HA (Bloomage Biotechnology Corp., Ltd.; 2000 kDa) and Dex with BDDE as a crosslinking agent (Sigma-Aldrich, St. Louis, MO, USA). HA and Dex (1:9 weight ratio (w/w) %) were mixed in 1.0 wt% NaOH (Sigma-Aldrich, USA) and stirred at low speed (80 rpm) at room temperature for 24 h to prepare a 10.0 wt% HA-Dex polymer solution. BDDE (0.5 wt%) was added to each concentration of HA-Dex polymer solution (10.0 wt%). The mix was poured into a molding frame and allowed to crosslink in a 50 °C water bath for 4 h. Then, the frame was removed to prepare the HA-Dex hybrid derivatives.

To make the CAE-loaded HA-Dex hybrid patches, BDDE (0.5 wt%) was added to HA-Dex polymer solution (10.0 wt%). The mix was poured into a molding frame and allowed to crosslink in a 50 °C water bath for 4 h. Then, CAE was added to each of the weight ratio samples. Then, varying amounts of CAE were added to produce five different hydrogel patches with the following proportions: control: HA-Dex hybrid hydrogel patches with no CAE; a: 9.8:0.2 HA-Dex: CAE; b: 9.6:0.4 HA-Dex: CAE; c: 9.4:0.6 HA-Dex: CAE; d: 9.2:0.8 HA-Dex: CAE; e: 9:1 HA-Dex: CAE (Table 1). The mixture was stirred until the CAE was completely embedded. The frame was removed to prepare CAE-loaded HA-Dex hybrid derivatives. The prepared derivatives were washed three to five times for 24 h using triple distilled water (DW, Milli-Q[®], USA) to remove any unreacted materials. Then, the CAE-loaded HA-Dex hybrid derivatives were lyophilized for 48 h in a freeze dryer (DFTtype, Ilshin Lab. Co., Ltd., Yangju-si, Korea) at −50 to −60 °C to prepare the CAE-loaded HA-Dex hybrid patches (Figure 2).

Table 1. Processing conditions for fabrication of CAE embedded HA-Dex hybrid patches.

Samples Weight Ratio (W/W)	HA-Dex Hybrid Patch *	CAE
Control	10.0	0
a	9.8	0.2
b	9.6	0.4
c	9.4	0.6
d	9.2	0.8
e	9.0	1.0

* Dextran: Hyaluronic acid (ratio) = 9.0:1.0.

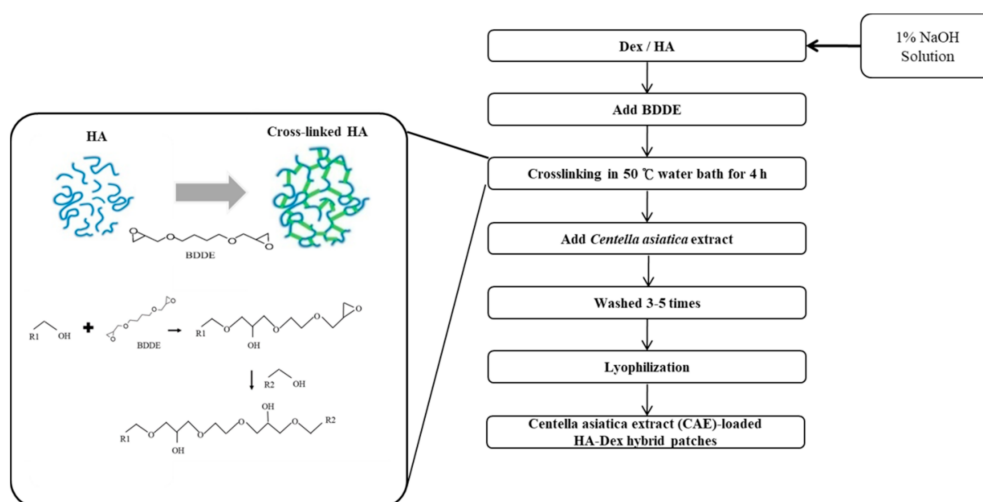


Figure 2. Schematic diagram showing the fabrication process of *Centella asiatica* extract (CAE)-loaded HA-Dex hybrid patches. Dextran (Dex, R1); hyaluronic acid (HA, R2).

2.2. Evaluation of Physical and Chemical Properties

Surface morphological analysis of the prepared patches was performed using a Field Emission Scanning Electron Microscope (FE-SEM) (Hitachi S-4300 & EDX-350, Hitachi, Chiyoda City, Japan). Patch porosity and porosity distribution were measured using a Procometer (Micromeritics AutoPore IV 9520, Norcross, GA, USA) and analyzed using an infrared spectrophotometer (FT-IR Spectrophotometer Frontier, PerkinElmer, Waltham, MN, USA). An Instron 5965 universal testing machine (UTM) was used to measure the tensile strength of the prepared patches.

2.3. Analysis of the Gelation Rate and Swelling Ratio

To measure the gelation rate of the CAE-loaded HA-Dex hybrid hydrogel patches, the initial weight (W_i) of the prepared patch was measured. Then, the patch was immersed in 50 mL ultrapure water and stirred in a shaking water bath (100 rpm) at 37 °C for 12 h. Afterward, the patch was placed in a freeze dryer. The dried weight (W_d) was measured and the gelation rate was calculated using Equation (1) [10], where

$$\text{Gelation rate (\%)} = W_d/W_i \times 100 \quad (1)$$

To calculate the swelling ratio, the initial dried weight (W_d) was measured after drying the patch at room temperature. The patch was then immersed in 50 mL ultrapure water and placed in a shaking water bath (100 rpm) at 37 °C for 24 h (W_s) until the absorption equilibrium of the patch was reached and the swelling ratio was calculated using Equation (2) [10], where

$$\text{Swelling ratio (\%)} = (W_s - W_d)/W_d \times 100 \quad (2)$$

2.4. Analysis of CAE Release Profile

To measure the CAE release profile, 10 mm × 10 mm patches were placed in a PBS solution (pH 7.2) and a drug release experiment was performed for 54 h in a shaking water bath (100 rpm) at 37 °C. A high performance liquid chromatography (HPLC) purification system (Prep 2535Q, Waters) was used to determine the concentration of released CAE every 4 h and analyze the drug release profile according to the changes in CAE concentration.

2.5. Cell Compatibility Analysis

The cytotoxicity of patch was estimated based on the international standard used for biological evaluation of medical device (ISO 10993-12 and ISO 10993-5) [17].

Briefly, 0.5 g of the patch sterilized by ethylene oxide gas was incubated in 50 mL of RPMI 1640 medium (BenchStable™ RPMI 1640, Gibco, Plymouth Meeting, PA, USA) containing 10% fetal bovine serum, 500 U/mL penicillin, and 500 µg/mL streptomycin (Gibco, USA) at 37 °C for 24 h under shaking. Afterwards, the patch extracts were filtered to remove insoluble material residues and sterilized by passage through a 0.2 µm filter. The cells were cultured at 37 °C in 5% CO₂ atmosphere for 3–5 days and 1×10^5 L929 (murine fibroblast cell line) cells were seeded into each well of 96-well culture plates. After 24 h, the culture medium was replaced by either fresh RPMI 1640 medium or patch extracts. Cells were then further incubated for 24 h. After replacing the old medium, cell counting kit-8 (CCK-8, Dojindo Laboratories, Kumamoto, Japan) was added to each well, and the cells were incubated for 4 h (37 °C, 5% CO₂). Absorbance at 450 nm was measured using an ELISA Reader (Infinite® 200 PRO, Tecan, Männedorf, Switzerland) to evaluate cell viability. Cell viability (%) was expressed as the relative absorbance of the sample to that of the control ($n = 3$, means ± SD).

2.6. Analysis of In Vitro Wound Closure

An in vitro wound closure model was used to analyze the atopic healing effect. We used the murine fibroblast cell line (L929 cells), which is commonly used in studies on skin regeneration, to verify the wound healing effects by analyzing time-dependent cell migration. RPMI 1640 medium

(BenchStable™ RPMI 1640, Gibco, PA, USA) containing 10% fetal bovine serum, 500 U/mL penicillin, and 500 µg/mL streptomycin (Gibco, USA) was used as the growth medium, and the cells were cultured at 37 °C in a 5% CO₂ incubator.

For the cell migration experiment, the L929 cells were grown in a 96-well plate, and when full growth was attained, wounds were created using pipette tip. A wound maker (pipette tip) was used to create a scratch in the cell monolayer. Cell migration was monitored for between 0 and 26 h and analyzed using a long-term cell image analysis program (Eclipse TI-E, Essen Bioscience, Ann Arbor, MI, USA). Healing time was measured as the time required for the cells to fill the damaged area.

2.7. Statistical Analysis

Data are expressed as the mean ± standard deviation (SD) of the mean. Collected data were evaluated using t-tests, and difference type data were evaluated using Sigma Plot Software (version 13, Systat Software, Inc., San Jose, CA, USA) and Microsoft Excel 2010 (Microsoft, Redmond, WA, USA).

3. Results and Discussion

3.1. Physical and Chemical Evaluation

BDDE binding of Dex, HA, and HA-Dex hybrids was analyzed using FT-IR spectra. The Dex -OH group was observed at 3200–3300 cm⁻¹. Moreover, at 1010 cm⁻¹, the COOH bond vibration intensity decreased as the HA concentration increased and the absorption peak decreased due to C-O-C contraction. This may be because -COOH (carboxyl group) underwent esterification to produce -COO through bonding, which resulted in an increased -C = O bond strength. The ester bond band was observed at 1709 cm⁻¹, confirming that the bond was formed by the crosslinking agent (Figure 3).

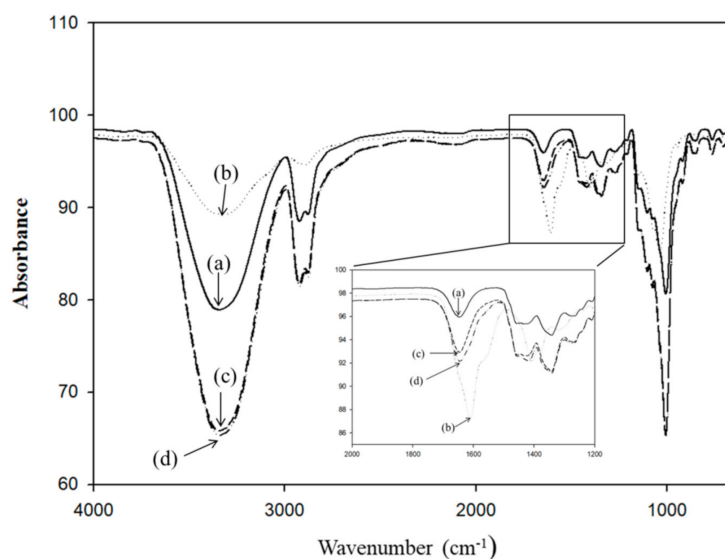


Figure 3. Fourier transform infrared spectra of hyaluronic acid-dextran (HA-Dex) hybrid hydrogel patches; (a) Dex, (b) HA, (c) Dex-HA (9.5:1.0), (d) Dex-HA (9.5:0.5).

FE-SEM analysis of the surface and a cross-section of the CAE-loaded HA-Dex hybrid hydrogel patches showed that the pore size decreased as the CAE content increased, and irregular pore shapes and surface distortions were observed (Figure 4).

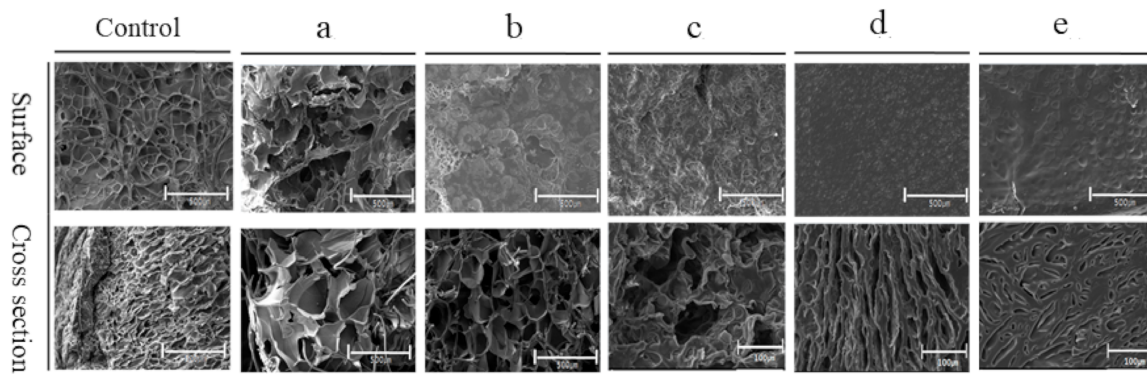


Figure 4. Morphologies of *Centella asiatica* extract-loaded hyaluronic acid-dextran hybrid patches by field emission scanning electron microscope analysis. Control: HA-Dex hybrid hydrogel patches with no CAE; (a) 9.8:0.2, (b) 9.6:0.4, (c) 9.4:0.6, (d) 9.2:0.8, and (e) 9:1 wt% HA-Dex: CAE (scale bars 5.0 kV × 5.0 K).

The porosity decreased slightly as the CAE concentration increased (Table 2).

Table 2. Porosity of *Centella asiatica* extract (CAE)-loaded hyaluronic acid-dextran (HA-Dex) hybrid hydrogel patches.

Patch Type	Total Intrusion Volume (Ml/G)	Total Pore Area (M ² /G)	Median Pore Diameter (Volume/Nm)	Median Pore Diameter (Area/Nm)	Average Pore Diameter (4V/A) Nm	Porosity(%)
a	1.6388	4.930	85,324.9	14.0	1329.6	68.2117
b	0.4233	0.943	16,078.3	77.7	1795.0	42.5677
c	0.4328	0.156	12,349.2	10,966.7	11,109.2	41.5143
d	0.3350	5.695	132,087.9	6.6	235.3	32.2406
e	0.2199	0.861	12,196.2	90.2	1021.8	26.5290

(a) 9.8:0.2, (b) 9.6:0.4, (c) 9.4:0.6, (d) 9.2:0.8, and (e) 9:1 wt% HA-Dex: CAE. Values are the mean of three measurements.

UTM measurements showed that the tensile strength increased as the CAE content increased, then decreased when CAE was added over 0.8 wt%. In addition, hydrated state hydrogels presented similar tensile properties when compared the different conditions. The dry state is the one where the CAE concentrations more affect the tensile properties of the hydrogels probably affected by the porosity. But nor in the hydrated state (Figure 5). Because, it may be that a greater number of holes on the surface and greater porosity led to decreased bonding strength due to pore–pore interaction, resulting in decreased tensile strength. In that case, decreased porosity would result in greater bonding strength, leading to increased tensile strength.

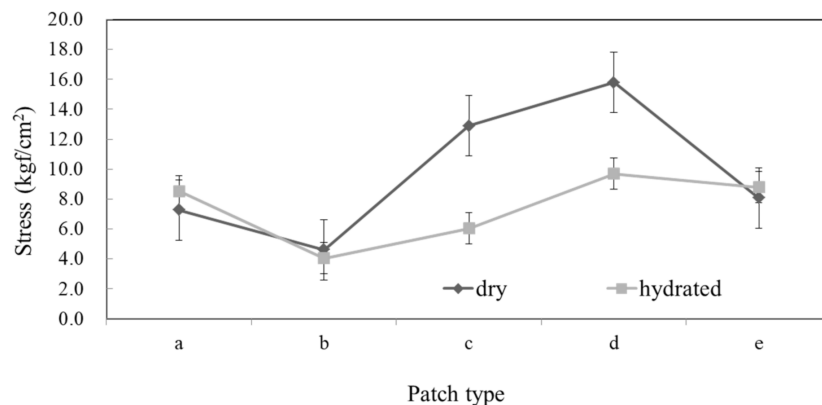
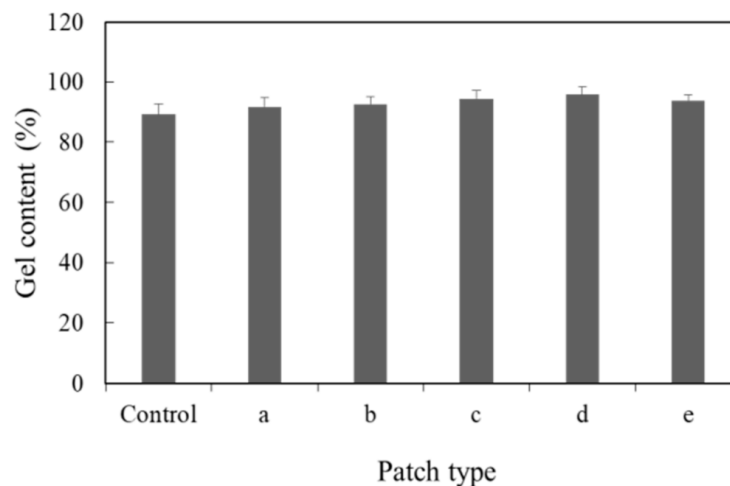


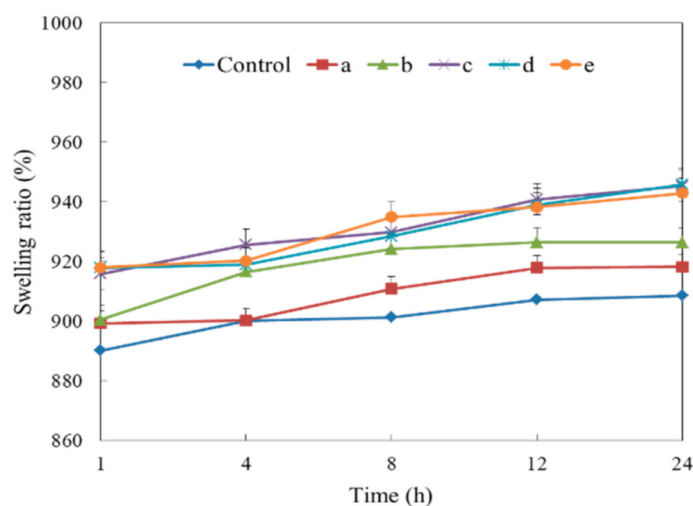
Figure 5. Tensile strength of *Centella asiatica* extract-loaded hyaluronic acid-dextran (HA-Dex) hybrid hydrogel patches ($n = 3$, mean \pm SD). Control: HA-Dex hybrid hydrogel patches with no CAE; (a) 9.8:0.2, (b) 9.6:0.4, (c) 9.4:0.6, (d) 9.2:0.8, and (e) 9:1 wt% HA-Dex: CAE.

3.2. Evaluation of Gelation Rate and Swelling Ratio

Comparison of patch gelation rates according to CAE concentration showed that all patches absorbed moisture after the patch was sufficiently swollen (12 h), and the gelation rates of all patch types were above 90% of the CAE concentration (Figure 6A). This high gelation rate could have resulted from the hydrophilicity of the HA and Dex polymers themselves and the porous structure of the hydrogel patch. In addition, CAE was sufficiently dissolved in the aqueous polymer solution, which led to increased water absorption. The swelling ratio tended to increase as the CAE concentration increased (Figure 6B).



(A)



(B)

Figure 6. Effect of *Centella asiatica* extract (CAE) on the characteristics of hyaluronic acid-dextran (HA-Dex) hybrid hydrogel patches. Effect of CAE content on (A) the gel content and (B) the swelling ratio ($n = 3$, mean \pm SD). Control: HA-Dex hybrid hydrogel patches with no CAE; (a) 9.8:0.2, (b) 9.6:0.4, (c) 9.4:0.6, (d) 9.2:0.8, and (e) 9:1 wt% HA-Dex: CAE.

3.3. Evaluation of the CAE Release Profile

The release profile of each type of CAE-loaded HA-Dex hybrid hydrogel patch was evaluated by HPLC analysis every 4 h. By 30 h, nearly all CAE had been released, although minor amounts of

CAE continued to be released until 54 h had elapsed (Figure 7). In particular, the release rate was significantly higher in patches containing 9.6:0.4 wt% HA-Dex: CAE. This is thought to be the result of the increased porosity of this patch type compared to those of the other groups. This would result in weaker bonding and a lower level of crosslinking.

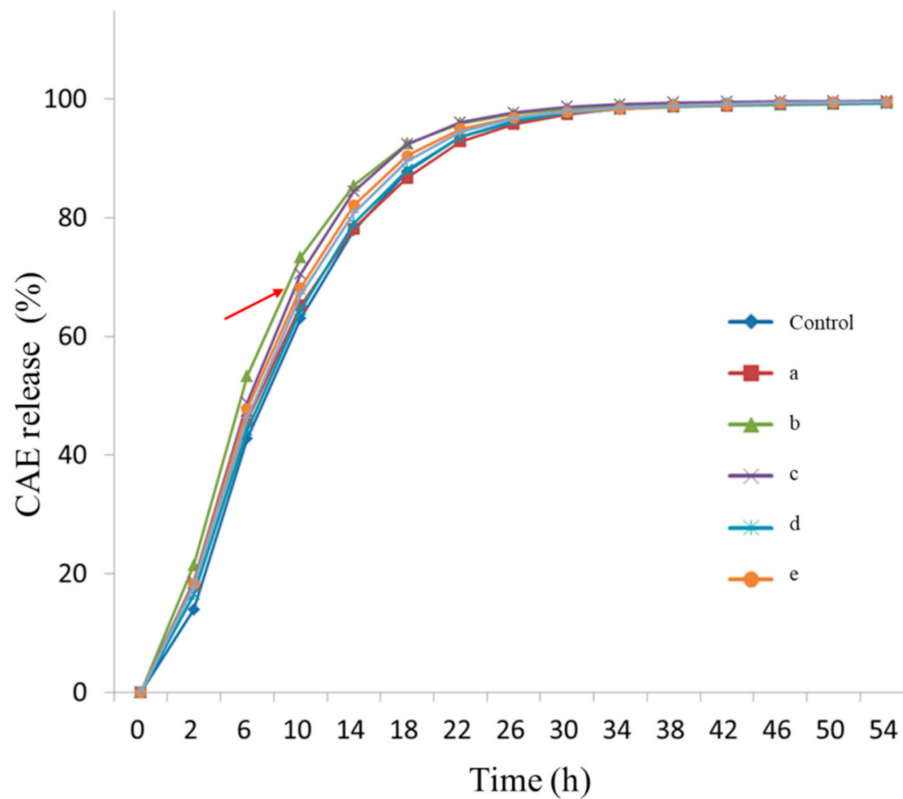
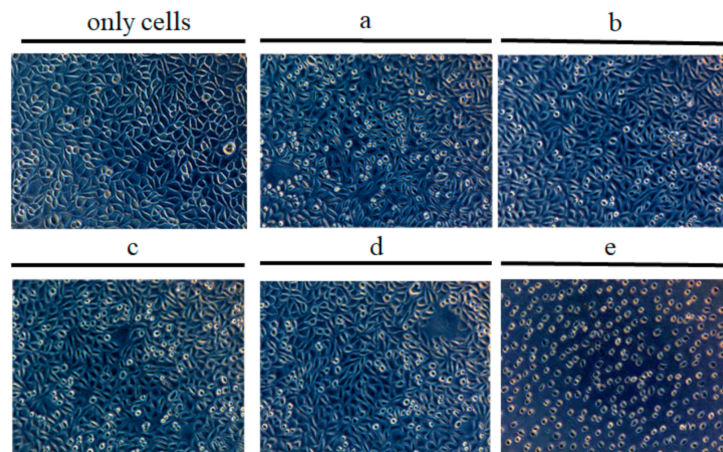


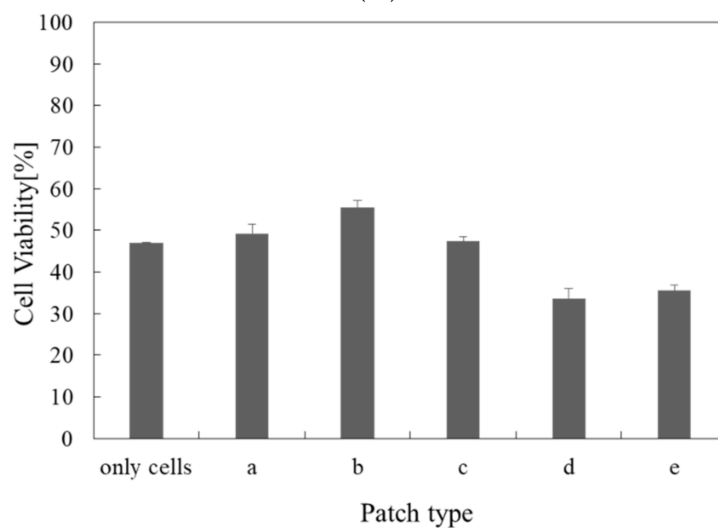
Figure 7. *Centella asiatica* extract (CAE) release profile of CAE-loaded hyaluronic acid-dextran (HA-Dex) hybrid hydrogel patches. Control: HA-Dex hybrid hydrogel patches with no CAE; (a) 9.8:0.2 HA-Dex: CAE; (b) 9.6:0.4 HA-Dex: CAE; (c) 9.4:0.6 HA-Dex: CAE; (d) 9.2:0.8 HA-Dex: CAE; (e) 9:1 HA-Dex: CAE.

3.4. Biocompatibility Evaluation

After removing the eluted medium, L929 cell growth in 96-well plates was observed using an optical microscope. Compared to untreated cells, cell shape was consistent, and cell viability was increased by the application of CAE-loaded HA-Dex hybrid hydrogel patches. However, when the CAE content was above a certain concentration, the number of cells decreased, and the size of the granules did not increase. Moreover, the shape of the cells was unstable, so the cells could not adhere, indicating decreased cell survival (Figure 8A). Cell viability was tested after obtaining the medium eluted from the L929 cells. Cell viability was similar to that of the untreated cells, but cell viability decreased above a 0.8 wt% CAE concentration (Figure 8B).



(A)



(B)

Figure 8. Biocompatibility of *Centella asiatica* extract (CAE)-loaded hyaluronic acid-dextran (HA-Dex) hybrid hydrogel patches. (A) Relative density and (B) relative viability of L929 cells treated with CAE-loaded HA-Dex hybrid patches ($n = 3$, mean \pm SD). (a) 9.8:0.2, (b) 9.6:0.4, (c) 9.4:0.6, (d) 9.2:0.8, and (e) 9:1 wt% HA-Dex: CAE.

3.5. Evaluation of In Vitro Wound Healing

Cell migration was measured over time as an indicator of wound healing. After 26 h, the wound had closed in almost all experimental groups. The rate of change in cell migration according to CAE release was similar in almost all experimental groups (Figure 9). However, cells treated with 9.6:0.4 wt% HA-Dex: CAE patches showed significantly more active migration, which led to decreased wound length. The optimal CAE concentration according to cell migration was 0.4 wt%.

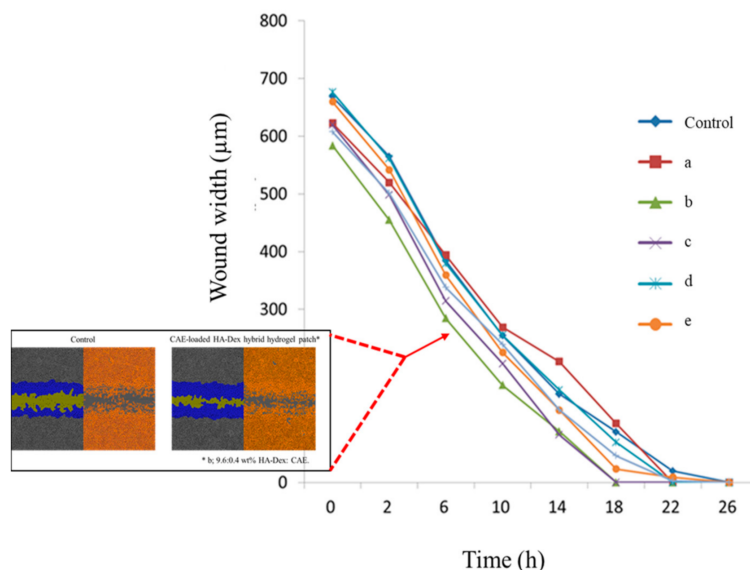


Figure 9. Wound closures rates for *Centella asiatica* extract (CAE)-loaded hyaluronic acid-dextran (HA-Dex) hybrid hydrogel patches. (a) 9.8:0.2, (b) 9.6:0.4, (c) 9.4:0.6, (d) 9.2:0.8, and (e) 9:1 wt% HA-Dex: CAE.

4. Conclusions

AD is a genetic disease involving immunological abnormalities. Studies suggest that a functional deficit due to a hypersensitization response caused by increased IgE antibody levels, disproportionate T lymphocyte differentiation resulting from decreased cell-mediated immune function, and skin adrenaline receptor blockages may cause AD. Moisturizing the surface of the skin and applying topical corticosteroids (a class of steroid hormones) are common approaches for treating or managing atopic diseases. However, the long-term use of hormonal agents causes various side effects including atrophied skin, vasodilation, pigmentation, and scarring [18]. Therefore, atopic treatments with anti-inflammatory properties that lack these side effects are needed.

This study successfully developed a CAE-loaded HA-Dex hybrid hydrogel patch that could control CAE release by fusing HA and DEX through a crosslinking agent (BDDE). FE-SEM showed that increased CAE content was associated with increasingly distorted pore sizes and shapes. In addition, the gelation rate, swelling ratio, and migration rate tended to increase as the CAE content increased. The highest level of cellular activity and the most stable release profile were obtained using a 0.4 wt% CAE-loaded HA-Dex hybrid hydrogel patch.

In conclusion, this enabled moisturization with minimal skin irritation even after a long period of use and the slow, stable release of CAE to the skin. The safety and efficacy of the patch for AD treatment were also evaluated in vitro. We found that patches containing 0.4 wt% CAE produced the most stable release profile and the highest level of cellular activity. This type of hydrogel patch could potentially be used as a delivery system for other therapeutic agents for AD.

Author Contributions: G.S.H. and J.H.C. conceived and designed the experiments; G.S.H. and J.Y.C. performed the experiments; G.S.H. and J.S.S. analyzed the data; J.H.C. and J.O.L. contributed reagents/materials/analysis tools; G.S.H. and J.Y.C. wrote the paper. All authors have read and agreed to the published version of the manuscript.

Funding: This research was funded by the Government-wide R&D Fund Project for Infectious Disease Research (GFID) (grant number: HG19C0707), Republic of Korea. Also this research was supported by the Ministry of SMEs and Startups(MSS), Korea, under the “Regional Specialized Industry Development Program (R&D, Project number P0013693)” supervised by the Korea Institute for Advancement of Technology (KIAT).

Acknowledgments: This research was supported by the Government-wide R&D Fund Project for Infectious Disease Research (GFID) (HG19C0707), Republic of Korea. Additionally, this research was supported by the Korea Institute of Industrial Technology (KITECH) under the “AI platform for vision systems and applications Project” (JA200003).

Conflicts of Interest: The authors declare no conflict of interest.

References

1. Park, Y.M. Advances in the pathophysiology of atopic dermatitis. *Pediatr. Allergy Respir. Dis.* **2006**, *16*, 189–196.
2. Patrizi, A.; Raone, B.; Raboni, R.; Neri, I. Efficacy and tolerability of a cream containing AR-GG27®(sorbityl furfural palmitate) in the treatment of mild/moderate childhood atopic dermatitis associated with pityriasis alba. A double-blind, placebo-controlled clinical trial. *G. Ital. Dermatol. Venereol.* **2012**, *147*, 1–8.
3. Garg, N.; Silverberg, J.I. Epidemiology of childhood atopic dermatitis. *Clin. Dermatol.* **2015**, *33*, 281–288. [[CrossRef](#)]
4. Myles, I.A.; Earland, N.J.; Anderson, E.D.; Moore, I.N.; Kieh, M.D.; Williams, K.W.; Saleem, A.; Fontecilla, N.M.; Welch, P.A.; Darnell, D.A.; et al. First-in-human topical microbiome transplantation with *Roseomonas mucosa* for atopic dermatitis. *JCI Insight* **2018**, *3*, 120608. [[CrossRef](#)] [[PubMed](#)]
5. Kyllönen, H.; Remitz, A.; Mandelin, J.M.; Elg, P.; Reitamo, S. Effects of 1-year intermittent treatment with topical tacrolimus monotherapy on skin collagen synthesis in patients with atopic dermatitis. *Br. J. Dermatol.* **2004**, *150*, 1174–1181. [[CrossRef](#)] [[PubMed](#)]
6. Ogawa, R. Keloid and hypertrophic scars are the result of chronic inflammation in the reticular dermis. *Int. J. Mol. Sci.* **2017**, *18*, 606. [[CrossRef](#)] [[PubMed](#)]
7. Young, H.T.; Choi, H.J. Clinical efficacy of functional herbal extracts liquid in atopic dermatitis patient. *Korean J. Food Nutr.* **2005**, *18*, 380–384.
8. Shon, M.Y.; Nam, S.H. Effect of *Eucommia ulmoides* extracts on allergic contact dermatitis and oxidative damage induced by repeat elicitation of DNCB. *J. Korean Soc. Food Sci. Nutr.* **2007**, *36*, 1517–1522. [[CrossRef](#)]
9. Adtani, P.N.; Narasimhan, M.; Punnoose, A.M.; Kambalachenu, H.R. Antifibrotic effect of *Centella asiatica* Linn and asiatic acid on arecoline-induced fibrosis in human buccal fibroblasts. *J. Investig. Clin. Dent.* **2017**, *8*, 12208. [[CrossRef](#)] [[PubMed](#)]
10. Lee, Y.; Choi, H.K.; N’deh, K.P.U.; Choi, Y.; Fan, M.; Kim, E.K.; Chung, K.H.; An, J.H. Inhibitory effect of *Centella asiatica* extract on DNCB-Induced atopic dermatitis in HaCaT cells and BALB/c mice. *Nutrients* **2020**, *12*, 411. [[CrossRef](#)] [[PubMed](#)]
11. Park, J.H.; Yeo, I.J.; Jang, J.S.; Kim, K.C.; Park, M.H.; Lee, H.P.; Han, S.B.; Hong, J.T. Combination effect of titrated extract of *Centella asiatica* and astaxanthin in a mouse model of phthalic anhydride-induced atopic dermatitis. *Allergy Asthma Immunol. Res.* **2019**, *11*, 548–559. [[CrossRef](#)] [[PubMed](#)]
12. Scott, J.F.; Conic, R.R.Z.; Kim, I.; Rowland, D.Y.; Nedorost, S.T. Atopy and sensitization to allergens known to cause systemic contact dermatitis. *Dermatitis* **2019**, *30*, 62–66. [[CrossRef](#)] [[PubMed](#)]
13. Kim, K.S.; Lee, Y.J.; Ryoo, W.S.; Noh, S.K. Preparation of high molecular weight atactic poly(vinyl alcohol) hydrogel by electron beam irradiation technique. *Polymer (Korea)* **2008**, *32*, 587–592.
14. Chen, J.; Jo, S.; Park, K. Polysaccharide hydrogels for protein drug delivery. *Carbohydr. Polym.* **1995**, *28*, 69–76. [[CrossRef](#)]
15. Hong, I.R.; Kim, Y.J. Self-Aggregated nanoparticles of lipoic acid conjugated hyaluronic acid. *Polymer (Korea)* **2008**, *32*, 561–565.
16. Kim, K.T.; Kim, Y.H.; Kim, J.G.; Han, C.S.; Park, S.H.; Kim, K.H. Preparation of oligo hyaluronic acid by hydrolysis and its application as a cosmetic ingredient. *J. Soc. Cosmet. Sci. Korea* **2007**, *33*, 189.
17. Wiegand, C.; Heinze, T.; Hipler, U.-C. Comparative in vitro study on cytotoxicity, antimicrobial activity, and binding capacity for pathophysiological factors in chronic wounds of alginate and silver-containing alginate. *Wound Repair Regen.* **2009**, *17*, 511–521. [[CrossRef](#)] [[PubMed](#)]
18. Grammatikos, A.P. The genetic and environmental basis of atopic diseases. *Ann. Med.* **2008**, *40*, 482–495. [[CrossRef](#)] [[PubMed](#)]

Publisher’s Note: MDPI stays neutral with regard to jurisdictional claims in published maps and institutional affiliations.



© 2020 by the authors. Licensee MDPI, Basel, Switzerland. This article is an open access article distributed under the terms and conditions of the Creative Commons Attribution (CC BY) license (<http://creativecommons.org/licenses/by/4.0/>).